

ADVANCES IN FOREST FIRE RESEARCH

2022

Edited by

**DOMINGOS XAVIER VIEGAS
LUÍS MÁRIO RIBEIRO**

Slope effect on Junction Fire with Two Non-symmetric Fire Fronts.

Carlos Ribeiro^{1*}; Domingos Viegas^{1;2}; Jorge Raposo^{1;2}; Luís Reis¹; Jason Sharples^{3;4}

¹ Association for the Development of Industrial Aerodynamics (ADAI)/Associated Laboratory on Energy, Transportation and Aeronautics (LAETA), University of Coimbra, Coimbra 3030-289, Portugal, {carlos.ribeiro, jorge.raposo, luis.reis}@adai.pt

² Department of Mechanical Engineering, University of Coimbra, Coimbra 3030-788, Portugal, {xavier.viegas@dem.uc.pt}

³ School of Science, University of New South Wales (UNSW), Canberra, ACT, Australia, {j.sharples@adfa.edu.au}

⁴ Bushfire and Natural Hazards Cooperative Research Centre, East Melbourne, VIC, Australia {j.sharples@adfa.edu.au}

*Corresponding author

Keywords

Junction Fires; Fire behaviour; Extreme Fire Behaviour; Merging Fires; Dynamic Fire behaviour

Abstract

The merging of two linear forest fire fronts that intersect at a small angle creates an accelerating fire in a relatively short time. In the majority of cases during the interaction, the fire fronts are non-symmetric. In Pedrogão Grande on the 17th June 2017, two-fire front merged and the propagation of the fire was influenced by the interaction of these two non-symmetric fire fronts. This forest fire motivates us to study the Junction Fire with two non-symmetrical fire fronts. The analysis of the interaction of two fire fronts and the angle between the bisector of the fire lines and the maximum ROS (γ) is of particular relevance. We found that with these preliminary laboratory tests, the non-ROS of intersection fire fronts for small rotation angles (δ) depends on the slope angle (α) and the initial angle between fire fronts. For the higher slope angles, the non-ROS is the highest influence by the convection process, and the angle γ where the maximum ROS occurred, increases when δ increases. However, for the lowest slope angles, the radiation process is dominant and influences the non-ROS. For these cases, the angle γ is near to the bisector of the fire lines.

1. Introduction

The merging of two fire fronts that intersect at a small angle induced very high values of the Rate of Spread (ROS) and fire intensity of their intersection point, and followed a gradual velocity decrease in the course of the time when the angle between fire fronts increases. This problem was studied in the past by Viegas et al. 2012, initially described this phenomenon as a Jump Fire, and developed a conceptual analytical model for the vertex “V” ROS. After the initial project, numerous research works experimental, analytical, and numerical simulation were followed (Viegas et al. 2013; Raposo et al. 2015, 2018; Sharples et al. 2013; Hilton et al. 2016; Thomas et al. 2017; Sullivan et al. 2019; Filkov et al. 2020). The fire fronts were always symmetrical in relation to the vertex “V” and there was no fuel bed to burn outside of linear straight fire lines. The results showed that the ROS of the vertex “V” has a great relationship in which the initial angle between the merging fire fronts and the ROS increases sudden zero to values of the order of one hundred times the basic ROS. A real fire situation occurred in the merging of two large fires: one near Canberra on the 18th January 2003 and, more recently, in Pedrogão Grande on the 17th June 2017.

On 17th June of 2017, the Pedrogão Grande fire starts at Escalos Fundeiros by 14:30h, and there was a second ignition in Regadas by 16:00h, local time, according to Viegas et al. 2017. The distances between those two ignitions were 2.6km and at 19:30h the two-fire front merged and the propagation of the fire was influenced by the interaction of these two non-symmetric fire fronts. This forest fire motivates us to study the Junction Fire with two non-symmetrical fire fronts.

2. Physical Problem

In the present study, it is assumed that two straight fire lines intersect at point A with an initial angle θ_0 between them and spread in a uniform fuel bed layer on a flat surface making an angle α with the horizontal datum $O_oX_oY_o$. Cartesian coordinate system $O_oX_oY_oZ_o$ is considered, in which O_oZ_o is perpendicular to the ground. Point A coincides initially with the origin of the reference cartesian frame with axis OX parallel to the slope gradient. The axis OX_1 represents the symmetry line of the fire configuration and can be defined by the angle δ that represents the angle between the bisector of the fire lines and the line with the highest slope. However, for each angle α and δ the maximum ROS happened according to axis OX_m and this axis is rotated some angle γ that represents the angle between the bisector of the fire lines and the maximum ROS. The fuel bed area is defined by ABC and is covered by a uniform layer of forest fuel able to support the spread of a surface fire. The merging of two linear fire fronts is illustrated schematically in Figure 1 a).

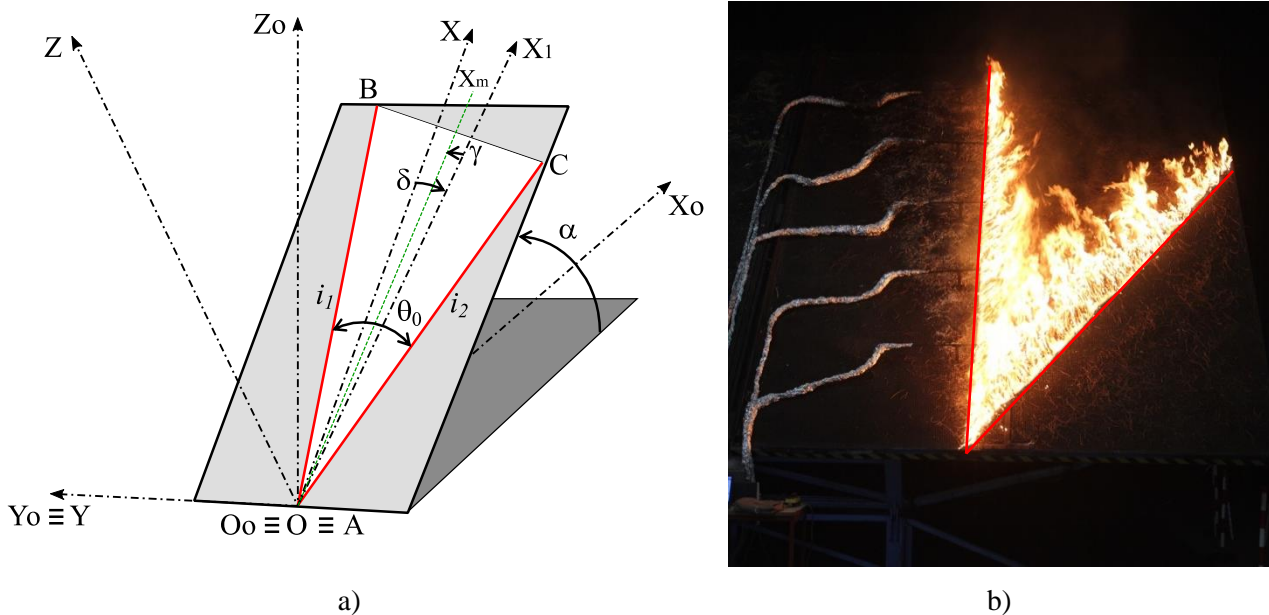


Figure 1- a) Schematic layout of the merging of two non-symmetric straight fire lines making an initial angle θ_0 between them. The axis OX is parallel to the slope gradient, the axis OX_1 represents the symmetry line of the fire configuration and the axis OX_m , defined by the green dashed line, represents the maximum ROS happened. b) View of the Canyon Table DE4 of the Forest Fire Laboratory of the University of Coimbra.

We consider two linear fire fronts defined by two straight lines (AB and AC), non-symmetric in the OX axis, as shown in Figure 1 a). Henceforward, the linear fire lines AB and AC will be referred to as i_1 and i_2 , respectively. In this study, it is assumed that the ambient air is still in accordance with the experimental conditions at the laboratory and at time $t_0=0s$, the fire lines are simultaneously and instantaneous ignited.

3. Material and Methods

3.1. Laboratory Experiments

Laboratory experiments were carried out at the Forest Fire Research Laboratory of the University of Coimbra using the Canyon Table DE4 and that has a useful area of $6.0 \times 8.0 m^2$ with a slope (α) that can be changed in the range of 0° to 40° . The initial angle θ_0 between the two fire lines was 30° . In Figure 1 b) typical performance conditions of these tests are shown.

During the preparation of each test, the conditions of the fuel load and bulk density were controlled, and the air temperature ($^\circ C$), relative humidity (%) and fuel moisture (m_f) were monitored. The fuel bed for the experiments was composed of dry particles of dead pine needles (*Pinus pinaster* - PP) with a constant load of $600 g \cdot m^{-2}$ (dry basis) (Viegas and Pita 2004; Xie et al. 2014; Raposo 2016; Raposo et al. 2018; Rodrigues et al. 2019; Viegas et al. 2021). The fuel bed height (h_f) was measured in five aleatory positions and on average it was 5.2cm. The basic rate of spread R_o ($cm \cdot s^{-1}$) of a linear fire front in a fuel bed with the same properties was measured for

each series of tests using a 1x1m² horizontal fuel bed without slope and wind. The ignition of the two fire lines was made by two persons to assure that the lines started burning simultaneously and two wool threads soaked in a mixture of petrol and diesel fuel were used. A summary of the main test parameters is provided in Table 1.

Table 1 – Parameters of the tests.

Ref.	Test	α (°)	δ (°)	m_f (%)	R_o (cm.s ⁻¹)
1	JF003030_2	30	15	13.90	0.203
2	JF052530_2	30	10	14.29	0.218
3	JF102030_2	30	5	14.29	0.221
4	JF003030_1	30	15	12.49	0.245
5	JF052530_1	30	10	12.49	0.245
6	JF003040_1	40	15	11.88	0.197
7	JF052540_1	40	10	13.64	0.263
8	JF102030_1	30	5	14.03	0.247
9	JF151530_1	30	0	13.64	0.209
10	JF151540_1	40	0	11.86	0.255
11	JF003010_1	10	15	13.25	0.226
12	JF003020_1	20	15	13.25	0.289
13	JF052510_1	10	10	13.25	0.276
14	JF052520_1	20	10	13.25	0.221
15	JF102010_1	10	5	13.25	0.267
16	JF102020_1	20	5	13.89	0.228
17	JF102040_1	40	5	14.81	0.220

3.2. Evolution of the ROS

The instantaneous position x_A of the intersection point A along the axis OX_m was the main object of the present analysis and it is associated with the overall evolution of the fire fronts. The displacement velocity R_A is defined as:

$$R_A = \frac{\partial x_A}{\partial t} \quad (1)$$

In order to compare results performed with different fuels we use the non-dimensional displacement velocity R'_A defined by:

$$R'_A = \frac{R_A}{R_o} \quad (1)$$

where R_o is the basic ROS.

4. Results and discussion

4.1. Rate of Spread analysis

The evolution of the fire front during tests performed was recorded by IR camera and frames with pre-defined times were used to measure the ROS of point A . The area between two fire fronts is burned by the advance of the intersection point A .

Results of R'_A from a series of tests performed as a function of the time are shown in Figure 2. In general, the evolution of R'_A , for $\alpha=10^\circ$ and $\alpha=20^\circ$, happens with a market acceleration when the fire lines are ignited, but, during the time, a deceleration phase happens. Otherwise, for $\alpha=30^\circ$ and $\alpha=40^\circ$, the evolution of R'_A has a market non-monotonic behaviour, but after the R'_A reaches the maximum value the deceleration phase happens. For the angle δ and slope angle α performed, there is no marked difference between the R'_A for each combination. For $\alpha=30^\circ$ and $\alpha=40^\circ$, the R'_A for $\delta=0^\circ$ (JF151530_1 and JF151540_1, respectively) on average during the time is quite similar to the δ values performed.

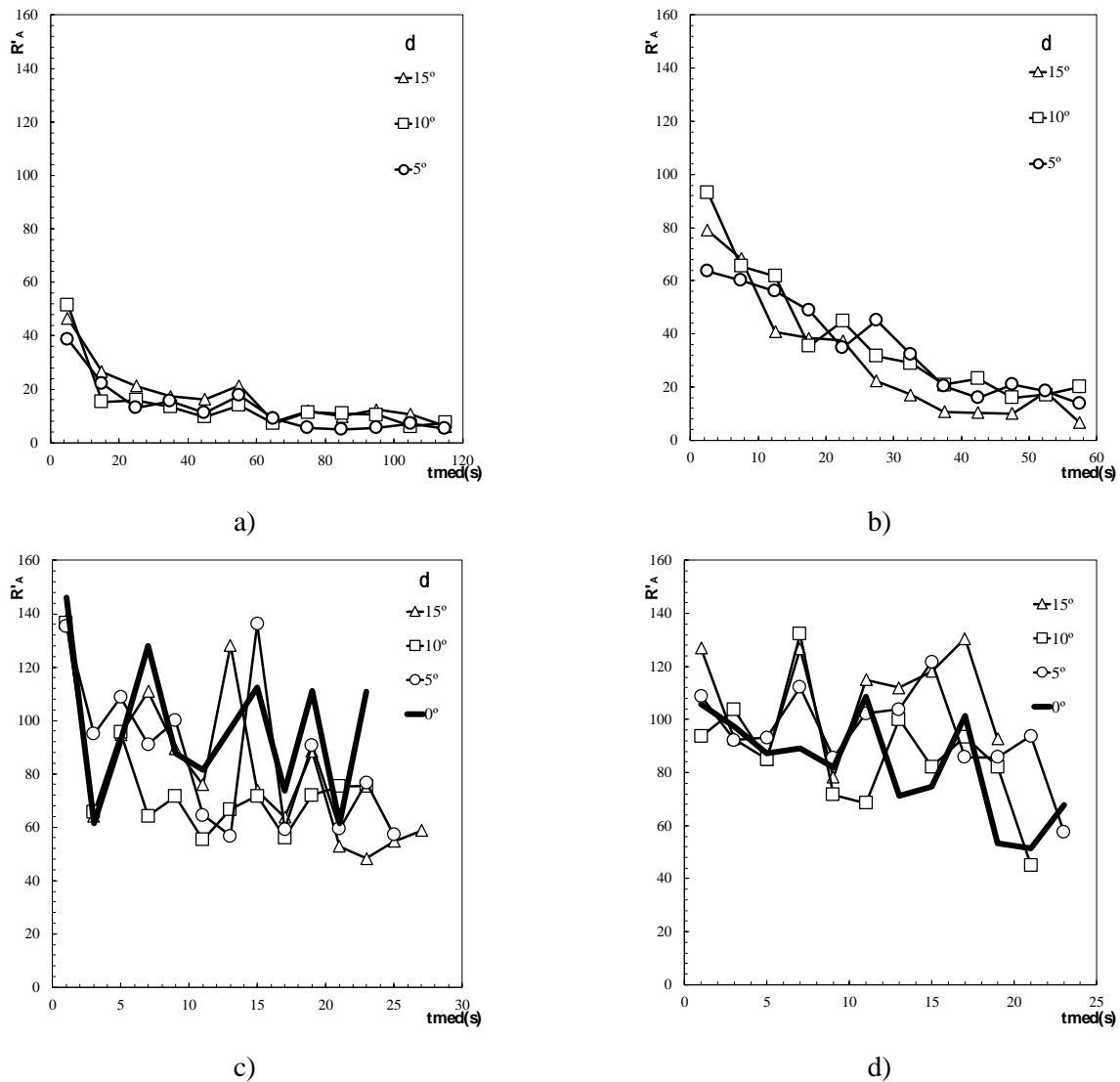


Figure 2 - Non-dimensional ROS R'_A of the intersection point A as a function of the time. The angle $\delta=5^\circ, 10^\circ$ and 15° were plotted in all analysis and, for $\alpha=30^\circ$ and 40° , the angle $\delta=0^\circ$ was added. a) $\alpha=10^\circ$; b) $\alpha=20^\circ$; c) $\alpha=30^\circ$ and d) $\alpha=40^\circ$

4.2. Angle of the maximum ROS

In order to assess the overall role of the parameters α and δ , the angle γ for each set of parameters was measured. These values are plotted in Figure 3 as a function of the angle between the bisector of the fire lines and the line with the highest slope (δ), for all tests performed. As can be seen, for the highest value of the slope ($\alpha=30^\circ$ and 40°) the angle γ has a similar trend and, in those cases, the axis, where happens the maximum ROS, is influenced more by the convection process. However, for the lower values of the slope the values ($\alpha=10^\circ$ and 20°) the angle γ tends to decrease and the maximum ROS happens near the bisector of the fire lines. In that case, the radiation process in the vicinity of point A is dominant relative to the convection process.

The dashed lines, in Figure 3, represent the fitted linear regression of the data values for each slope angle (α) and the correlation coefficient R^2 for this fitting is for $\alpha=10^\circ$, $R^2=0.864$, and $\alpha>10^\circ$, $R^2=0.991$.

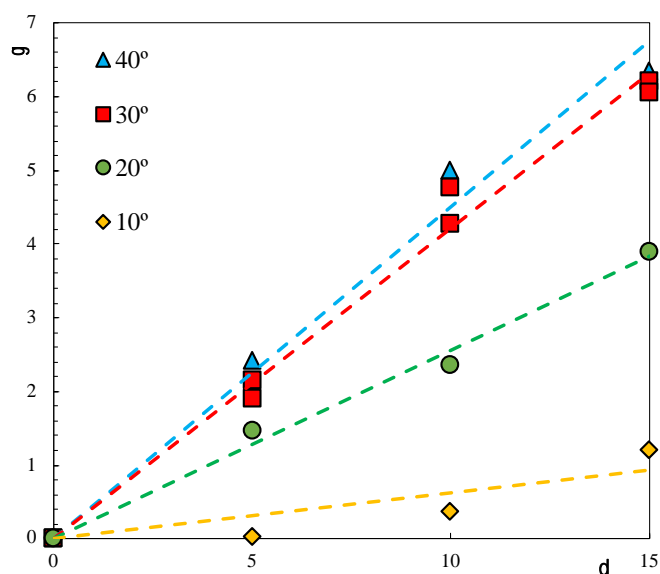


Figure 3- The angle between the bisector of the fire lines and the maximum ROS (γ) as a function of the angle between the bisector of the fire lines and the line with the highest slope (δ). The dashed lines represent the fitted linear regression of the data values for each slope angle (α).

5. Conclusion

Analysis of the Junction Fires with non-symmetric linear fire lines based on laboratory scale experiments was performed for different inclined terrain, $\alpha=10^\circ$, 20° , 30° and 40° . The evolution of the fire front consists mainly of the advance of the intersection point A, with an initial angle $\theta_0=30^\circ$ between fire lines. For the δ angles performed, the non-ROS R'_A is quite similar for each slope angle and, for $\alpha=30^\circ$ and 40° , similar with symmetric condition $\delta=0^\circ$. With these preliminary laboratory tests, we conclude that the non-ROS of the intersection point A for small rotation angles depends on the slope angle and the initial angle of the fire fronts. However, for the highest slope angles, the convection process is dominant and changes the angle γ where the maximum ROS occurred but, for the lowest slope angles, the variation angle γ is lower and near to the bisector of the fire lines.

This study must be complemented by more tests to reduce experimental errors and to explore other conditions, different fuel bed types and scale effects.

6. References

- Filkov A, Cirulis B, Penman T (2020) Quantifying merging fire behaviour phenomena using unmanned aerial vehicle technology. *International Journal of Wildland Fire*. doi:10.1071/WF20088.
- Hilton JEA, Miller CA, Sharples JJB, Sullivan ALC (2016) Curvature effects in the dynamic propagation of wildfires. *International Journal of Wildland Fire* 2016, 25, 1238–1251. doi:10.1071/WF16070.
- Raposo JR, Cabiddu S, Viegas DX, Salis M, Sharples J (2015) Experimental analysis of fire spread across a two-dimensional ridge under wind conditions. *International Journal of Wildland Fire*. doi:http://dx.doi.org/10.1071/WF14150.
- Raposo JRN (2016) Extreme Fire Behaviour Associated to Merging of Two Linear Fire Fronts. Coimbra. http://hdl.handle.net/10316/31020.
- Raposo JR, Viegas DX, Xie X, Almeida M, Figueiredo AR, Porto L, Sharples J (2018) Analysis of the physical processes associated with junction fires at laboratory and field scales. *International Journal of Wildland Fire* 27, 52–68. doi:10.1071/WF16173.
- Rodrigues A, Ribeiro C, Raposo J, Viegas DX, André J (2019) Effect of canyons on a fire propagating laterally over slopes. *Frontiers in Mechanical Engineering* 5, 402–409. doi:10.14195/978-989-26-16-506_43.
- Sharples JJ, Cary GJ, Fox-Hughes P, Mooney S, Evans JP, Fletcher MS, Fromm M, Grierson PF, McRae R, Baker P (2016) Natural hazards in Australia: extreme bushfire. *Climatic Change* 139, 85–99. doi:10.1007/s10584-016-1811-1.

- Thomas CM, Sharples JJ, Evans JP (2017) Modelling the dynamic behaviour of junction fires with a coupled atmosphere–fire model. *International Journal of Wildland Fire* 26, 331–344. doi:10.1071/WF16079.
- Viegas DX, Pita LP (2004) Fire spread in canyons. *International Journal of Wildland Fire* 13, 253. doi:10.1071/WF03050.
- Viegas DX, Raposo JR, Davim D a., Rossa CG (2012) Study of the jump fire produced by the interaction of two oblique fire fronts. Part 1. Analytical model and validation with no-slope laboratory experiments. *International Journal of Wildland Fire* 21, 843–856. doi:http://dx.doi.org/10.1071/WF10155.
- Viegas D, Raposo J, Figueiredo A (2013) Preliminary analysis of slope and fuel bed effect on jump behavior in forest fires. *Procedia Engineering* 62, 1032–1039. doi:10.1016/j.proeng.2013.08.158.
- Viegas DX, Almeida M, Ribeiro L, Raposo J, Viegas MT, Oliveira R, Alves D, Pinto C, Humberto J, Rodrigues A, Lucas D, Lopes S, Silva L (2017) O COMPLEXO DE INCÊNDIOS DE PEDRÓGÃO GRANDE E CONCELHOS LÍMITROFES, INICIADO A 17 DE JUNHO DE 2017. (Coimbra, Portugal)
- Viegas D, Raposo J, Ribeiro C, Reis L, Abouali A, Viegas CX (2021) On the non-monotonic behaviour of fire spread. *International Journal of Wildland Fire*. doi:10.1071/WF21016.
- Xie X, Liu N, Viegas DX, Raposo JR (2014) Experimental Research on Upslope Fire and Jump Fire. *Fire Safety Science* 11, 1430–1442. doi:10.3801/IAFSS.FSS.11-1430.